ChemCatChem 4 (2012) 1764-1775

Ga-Pd/Ga_2O_3 Catalysts: The Role of Gallia Polymorphs, Intermetallic Compounds, and Pretreatment Conditions on Selectivity and Stability in Different Reactions

L. Li,[a,b,c] B. Zhang,[b] E. Kunkes,[b] K. Föttinger,[d] M. Armbrüster,[e] D. S. Su,[b] W. Wei,[a] R. Schlögl,[b] M. Behrens[b,*]

[1] State Key Laboratory of Coal Conversion, Institute of Coal Chemistry, Chinese Academy of Sciences, Taiyuan, 030001 (PR China)
[2] Department of Inorganic Chemistry, Fritz-Haber-Institut der Max-Planck-Gesellschaft, Faradayweg 4–6, 14195 Berlin (Germany)
[3] Graduate University of Chinese Academy of Sciences, Beijing, 100049, (PR China)
[4] Institute of Materials Chemistry, Vienna University of Technology, Getreidemarkt 9, 1060 Vienna (Austria)
[5] Max-Planck-Institut für Chemische Physik fester Stoffe, Nöthnitzer Str. 40, 01187 Dresden (Germany)

[*] Corresponding author: e-mail behrens@fhi-berlin.mpg.de,

Received 25 April 2012; Article first published online: 30 August 2012; Published November 2012

Abstract

A series of gallia-supported Pd-Ga catalysts that consist of metallic nanoparticles on three porous polymorphs of Ga_2O_3 (α-, β-, and γ-Ga_2O_3) were synthesized by a controlled co-precipitation of Pd and Ga. The effects of formation of Ga-Pd intermetallic compounds (IMCs) were studied in four catalytic reactions: methanol steam reforming, hydrogenation of acetylene, and methanol synthesis by CO and CO_2 hydrogenation reactions. The IMC Pd_2Ga forms upon reduction of α- and β-Ga_2O_3-supported materials in hydrogen at temperatures of 250 and 310 °C, respectively. At higher temperatures, Ga-enrichment of the intermetallic particles is observed, leading to formation of Pd_5Ga_3 before the support itself is reduced at temperatures above 565 °C. In the case of Ga-Pd/γ-Ga_2O_3, no information about the metal particles could be obtained owing to their very small size and high dispersion; however, the catalytic results suggest that the IMC Pd_2Ga also forms in this sample. Pd_2Ga/gallia samples show a stable selectivity towards ethylene in acetylene hydrogenation (≈75 %), which is higher than for a monometallic Pd reference catalyst. An even higher selectivity of 80 % was observed for Pd_5Ga_3 supported on α-Ga_2O_3. In methanol steam reforming, the Ga-Pd/Gallia catalysts showed, in contrast to Pd/Al_2O_3, selectivity towards CO_2 of up to 40 %. However, higher selectivities, which have been reported for Pd_2Ga in literature, could not be reproduced in this study, which might be a result of particle size effects. The initially higher selectivity of the Pd_5Ga_3-containing samples was not stable, suggesting superior catalytic properties for this IMC, but that re-oxidation of Ga species and formation of Pd_2Ga occurs under reaction conditions. In methanol synthesis, CO hydrogenation did not occur, but a considerable methanol yield from a CO_2/H_2 feed was observed for Pd_2Ga/α-Ga_2O_3.

Keywords: gallium; hydrogenation; intermetallic phases; palladium; reduction

1. Introduction

Pd is an element that is widely applied in heterogeneous catalysis. It is, e.g., active in various hydrogenation and reforming reactions. It is known that the catalytic properties of Pd metal can be modified by alloying or formation of intermetallic compounds (IMCs).[1] The latter is in particular interesting, if the selectivity to a desired product can be improved without losing the typical high activity of Pd. Alteration of the catalytic properties can be either understood in terms of a modified electronic structure[2-5] or by a geometrical site isolation at the IMC's surface.[6-8]

In the case of Pd-based IMCs, unsupported Ga-Pd IMCs have been investigated regarding their intrinsic catalytic properties and dramatic differences compared to monometallic Pd catalysts have been observed.[1,9-12] The selectivity towards ethylene in the semi-hydrogenation of acetylene was reported to be higher and more stable at conditions where a pure Pd catalyst produced mainly ethane. This effect has been attributed to site-isolation of the active Pd atoms by increasing Pd-Pd distances and reducing Pd-

Pd coordination numbers on the catalyst surface affects their adsorbing abilities[13] as well as a modification of the electronic structure of the material. The Ga-Pd IMCs studied in the aforementioned publications are prepared by melting the corresponding amounts of Pd and Ga in a high frequency induction furnace and subsequent annealing at high temperature in inert atmosphere to obtain single-phase Ga-Pd IMCs. This approach is very useful to study the intrinsic properties of these model materials, but it sacrifices surface area. Chemical etching have been proposed to increase the surface area, but lead to a partial decomposition of the IMCs structure and a Pd-enriched surface with decreased selectivity.[12,14,15]

Supported Pd-Ga IMCs nanoparticles have been reported to be accessible by Pd-impregnation of Ga_2O_3[16,17] followed by co-reduction, preparation in organic phase,[18] from co-precipitated hydrotalcite-like precursors[19] and by co-impregantion of Pd and Ga on carbon nanotubes.[15] Co-precipitation was in particular suited for the preparation of very small and uniform Pd_2Ga particles. Here, we present a simple aqueous and robust synthesis of nanocrystalline Ga-Pd IMCs that is based on co-precipitation of Pd^{2+}/Ga^{3+} solution to yield Ga_2O_3 in different polymorphs,[20] α-, β- and γ-Ga_2O_3 with a homogeneous distribution of Pd-species. We have studied the formation of Ga-Pd IMCs in reducing atmosphere and present the effect of Gallia modification on IMC formation. The resulting catalysts were characterized using various bulk and surface sensitive methods. We use four important test reactions to study the catalytic properties of the samples, where monometallic Pd is known to be active and selectivity is a major issue. These are acetylene hydrogenation, methanol steam reforming (MSR) and methanol synthesis by CO and CO_2 hydrogenation. Special attention was paid to the modification of the catalytic properties with IMC formation and composition and to the question whether the formed Ga-Pd IMCs maintain these modifications in the chemical potential of the different feed gases

2. Results and Discussion

2.1. Synthesis and characterization of PdO/gallia materials

To obtain the Ga-Pd IMC nanoparticles with uniform size supported on α-, β- and γ-Ga_2O_3, we have used co-precipitation of a mixed solution of Ga and Pd nitrate with sodium carbonate to prepare the precursors with homogeneous distribution of Pd and Ga. Syntheses were based on the optimal preparation conditions for the different Ga_2O_3 modifications in aqueous solution described in our previous study.[20] The only modification to the synthesis presented therein was that for this study Pd^{2+} has been added to the starting solution to give a molar Ga:Pd ratio of 98:2, resulting in a 2 wt-% loading based on Pd/Ga_2O_3. A detailed description of the co-precipitates and their thermal properties are given as supporting information. PdO/α-Ga_2O_3 and PdO/β-Ga_2O_3 have been prepared by calcinations of an α-GaOOH precursor at different temperatures, while PdO/γ-Ga_2O_3 was obtained from an amorphous precursor. Presence of the different gallia modifications after calcination have been confirmed by XRD (Fig. 1a,c,e).

Table 1. N_2 physisorption results for the calcined samples. For comparison those of the Pd-free samples from ref [20] are given in parentheses.

Sample	T_{calc} / °C	BET-SA / m^2/g	Pore volume / cm^3/g	Pore diameter[a] / nm
PdO/α-Ga_2O_3	400	70 (55)[b]	0.13 (0.14)[b]	7 (10)[b]
PdO/β-Ga_2O_3	800	25 (23)[c]	0.091 (0.15)[c]	15 (25)[c]
PdO/γ-Ga_2O_3	500	91 (116)	0.35 (0.19)	15 (7)

[a] from BJH analysis. [b] Pd-free sample was calcined at 350 °C. [c] Pd-free samples was calcined at 700 °C.

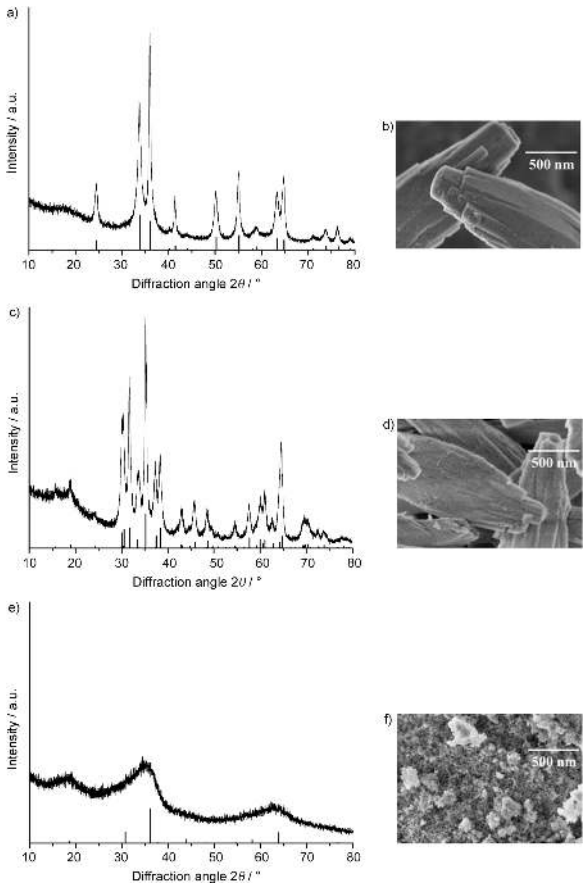

Figure 1. XRD and SEM of calcined samples. The histograms in (a), (c) and (e) represent α-Ga_2O_3, β-Ga_2O_3 and γ-Ga_2O_3 with ICSD Nr. 27431, 83645 and 152085, respectively. The differences in relative peak intensities between the experimental and literature data in a) can be explained with preferred orientation of the anisotropic crystallites.

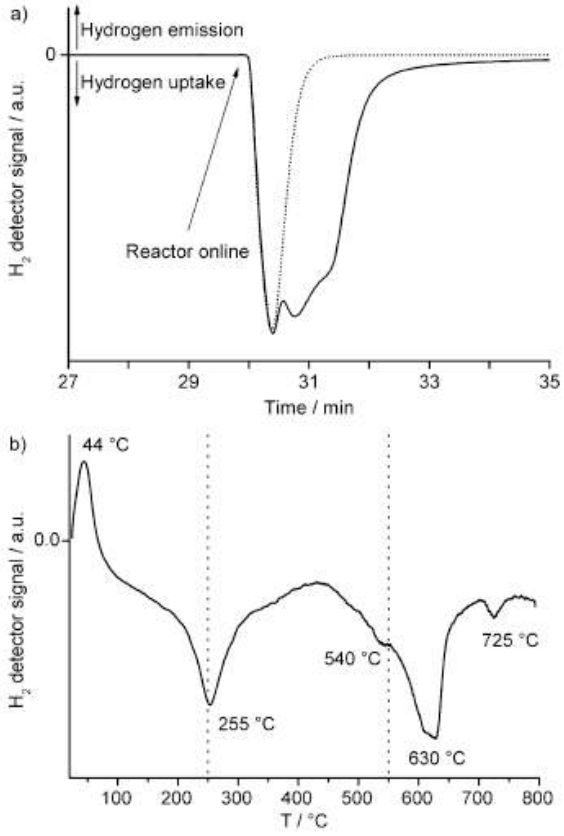

Figure 2. Reduction of the PdO/a-Ga_2O_3 sample. a) The hydrogen detector signal at RT versus time for an empty reactor (**.....**) and the reactor containing the sample (−−−). The detector background signal was substracted. Independent of sample reduction, the amount of pre-filled Ar that is purged out of the reactor leads to a signal also for the empty reactor. The difference between (**.....**) and (−−−) is assigned tot he interaction of hydrogen with Pd (see text). (b) The hydrogen detector signal is shown during TPR. The positive signal corresponds to hydrogen evolution as a result of thermal decomposition of Pd hydride and negative signals correspond to hydrogen consumption. The dotted vertical lines correspond to the reduction temperatures used for catalyst preparation.

The textural properties of the three samples were found to be similar to those reported previously for the pure gallia polymorphs[20] and are reported in Table 1. As a first indication of homogenous Pd distribution, no crystalline PdO could be detected by XRD and the color of the materials was yellow rather than brown as would be expected for bulk-PdO. In agreement with the pure Gallia samples,[20] SEM investigation revealed differences in particle morphology (Fig. 1b,d,f). α-Ga_2O_3 and β-Ga_2O_3 have been prepared from micrometer-sized α-GaOOH particles and the "rice grain-like" morphology of the precursor aggregates[20] has been conserved upon calcination at 400 °C (α-phase, Fig. 1b) and 800 °C (β-phase, Fig, 1d). Larger pores are present at the surface of the β-phase after calcination at higher temperature. In contrast, the mostly amorphous γ-Ga_2O_3, which posseses the highest specific surface area (Table 1), exhibits aggregates of very small nanoparticles (<10 nm)[20] after calcination at 500 °C (Fig. 1f).

2.2. Formation of Ga-Pd IMCs

The IMC formation upon reduction of the calcined samples is discussed in detail for the Pd/α-Ga_2O_3 system in the following, detailed information on the β- and γ-Ga_2O_3 samples can be found at the end of this section and as supplementary data. Upon feeding of diluted hydrogen over the material at room temperature, hydrogen consumption occurred instantaneously (Fig. 2a). The H_2 consumption at room temperature is 0.24 mmol/g_{cat}, which is higher than 0.17 mmol/g_{cat} expected for stoichiometric reduction PdO to Pd metal. This difference as well as the shoulder in the TPR profile is attributed to formation of PdH_x.[16,21,22] Also spill-over of hydrogen to the support material may contribute.[23-25] TPR experiments were conducted and are displayed in Fig. 2b. With increasing temperature, PdH_x is decomposed around 44 °C, giving a positive peak of the hydrogen detector.

Two appreciable hydrogen consumption peaks possibly related to the reduction of gallium species appear around 255 and 630 °C with a H_2 consumption of 0.16 and 0.21 mmol/g_{cat}, respectively. Pure α-Ga_2O_3 cannot be reduced with H_2 at a temperature less than 627 °C,[20,26] indicating that the addition of Pd effectively promotes the reduction of the α-Ga_2O_3 support. This is attributed to the ability of Pd to activate di-hydrogen and then spill very reactive atomic hydrogen over onto the Ga_2O_3 support.[27] It is know that under reducing conditions Ga-Pd IMCs can be formed from PdO/gallia samples.[23,28] Assuming IMC formation as the only reason for hydrogen consumption, the formal Pd^0:Ga^0 ratio of the product would be $Pd_{1.5}Ga$ after step 1 and $Pd_{1.4}Ga$ after step 2. However, this consideration does not involve partial reduction of Ga_2O_3 with Ga^{d+} species of intermediate oxidation state (d < 2),[17,29,30] which becomes likely at high temperatures. Thus, the real Ga content of the formed IMCs is probably lower. The TPR data suggests that after room temperature reduction of PdO and Pd-hydride decomposition a Pd-rich IMC is formed during reduction step 1 at approximately 250 °C and that step 2 at 630 °C is most likely due to further (partial) reduction of the Ga_2O_3 support. Additional weaker TPR signals are detected at 540 and 725 °C, which also might be related to formation of Ga-Pd IMCs with increasing Ga-content.

To get more insight into the IMC formation at higher temperature, the TPR experiment of PdO/α-Ga_2O_3 was simulated at the ambient pressure XPS beamline ISSIS at BESSY-II (Berlin) in 1 mbar H_2 with a constant heating rate of 2 °C/min up to a temperature of 513 °C, which was chosen as a limit to avoid pronounced evaporation of Ga species into the reaction chamber. To obtain information for both Ga 3d and Pd 3d core levels from the same penetration depth, different excitation energies of the X-ray beam were chosen (Ga 3d: 396 eV and Pd 3d: 720 eV) to

achieve similar kinetic energy of the produced photoelectrons. Due to severe sample charging at low temperature, high quality data could only be obtained at temperature > 300 °C. Fig. 3a exemplifies the Ga 3d binding energy region. The spectrum was recorded at 317 °C and the main signal at 20.55 eV is assigned to Ga^{3+} from the α-Ga_2O_3 support.[17,29-33] Its position remained unchanged, irrespective of temperature. A broad O 2s signal also originating from the Ga_2O_3 support was additionally observed at 23.65 ± 0.1 eV, and found to be independent of temperature.[33] Two other signals are recorded at 19.0 ± 0.2 eV and 18.35 ± 0.1 eV. The intermetallic compound PdGa shows a doublet signal with a stronger component at approximately 18.5 eV and another one at 19.0,[11] but overlaps with that of a partially reduced Ga^{d+} species that is found in Gallia under reducing conditions and makes it difficult to resolve the doublet. In this work, the positions and half-widths of two peaks have been determined in the spectrum taken at the highest reduction temperature (at 19.0 ± 0.2 eV and 18.35 ± 0.1 eV with FWHM = 1.1 ± 0.1 eV and 0.8 ± 0.1 eV, respectively) and kept constant during fitting of the other spectra. The two signals are assigned to $Ga^{\delta+}$ and (inter)metallic Ga^0, respectively.[17,29-31] The absolute values for the surface concentration and peak positions of the reduced Ga species resulting from this evaluation have to be treated with care, because the low amount of these species in comparison with Ga^{3+} and the uncertainties due to peak overlapping lead to large errors. However, despite significant data scattering some clear trends can be observed during the in-situ experiment, which are regarded to be reliable on a semi-quantitative basis.

The Pd 3d region at 308 °C is shown in Fig. 3b. Already at this temperature, a significant modification of the Pd electronic state compared to metallic Pd was observed: The Pd $3d_{5/2}$ peak is shifted by 0.9 eV to higher binding energy. This observation is consistent with previous studies of Ga-Pd IMCs,[11] in which filling of the valence d band of Pd was explained by covalent interactions between Pd and Ga. On basis of the core level integrals a Pd^0:Ga^0 ratio near 2:1 was determined for the lowest reduction temperature of the XPS study (Fig. 3c). Considering that this temperature already exceeds the first TPR signal, there is good agreement between XPS and TPR indicating that the IMC Pd_2Ga was formed during reduction step 1. As the reduction temperature was increased to ca. 450 °C, a slow and gradual Ga-enrichment of the IMC was detected down to a total Pd^0:Ga^0 ratio close to 1:1. Simultaneously, a shift of the Pd $3d_{5/2}$ binding energy to 336.15 ± 0.1 eV was detected indicating that at least part of the newly reduced Ga interacts with the Pd species in the IMC. This corresponds to the temperature regime between the two TPR peaks, where no clear reduction signals have been detected (Fig. 2b). Thus, contrary to the initial formation of Pd_2Ga, further Ga enrichment of the IMC towards phases like Pd_5Ga_3,or PdGa does not seem to be associated with a well-resolved reduction step, but seem to be rather a gradual process, which involves continuous H_2 consumption. Starting from approx

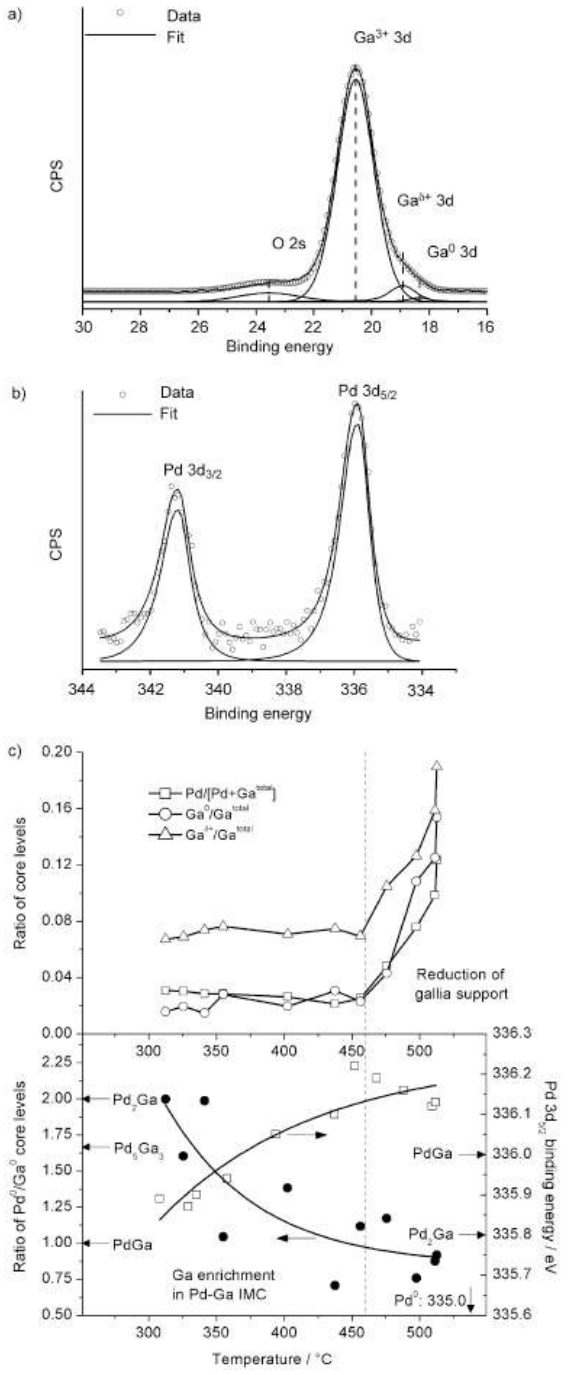

Figure 3. Examples of a) Ga3d and b) Pd3d in situ core level XPS spectra of the Pd/α-Ga_2O_3 during reduction with data fitting. CPS=counts per second. c) Dynamic changes in the XPS spectra over the temperature range between approximately 300 and 500 °C.

imately 450 °C a strong increase in Ga^{d+} and Ga^0 concentration was detected, but now without pronounced further change of the Pd^0:Ga^0 ratio or the Pd $3d_{5/2}$ binding energy (Fig. 3c). This simultaneous enrichment of reduced Ga species and Pd at the surface is ascribed to the beginning evaporation of volative Ga(I) species. This temperature regime corresponds to the onset of the second reduction step observed in TPR, which now can be assigned to the

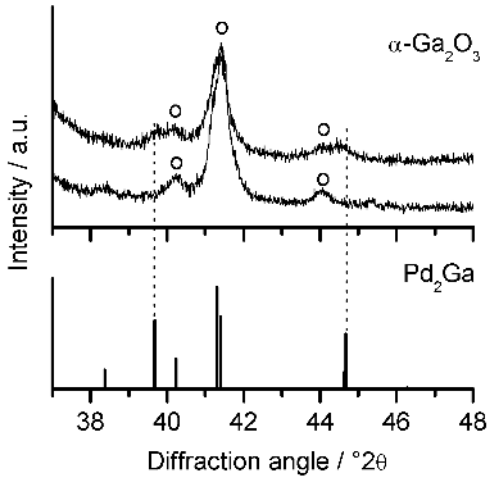

Figure 4. Enlarged sections of the XRD patterns of PdO/a-Ga_2O_3 after reduction at a) 250 and b) 550 °C. Although the peaks of the gallia support did not changed in comparison to the calcined samples (Figure 1), new peaks appeared at positions expected for the Pd_2Ga IMCs in the sample reduced at 250 °C

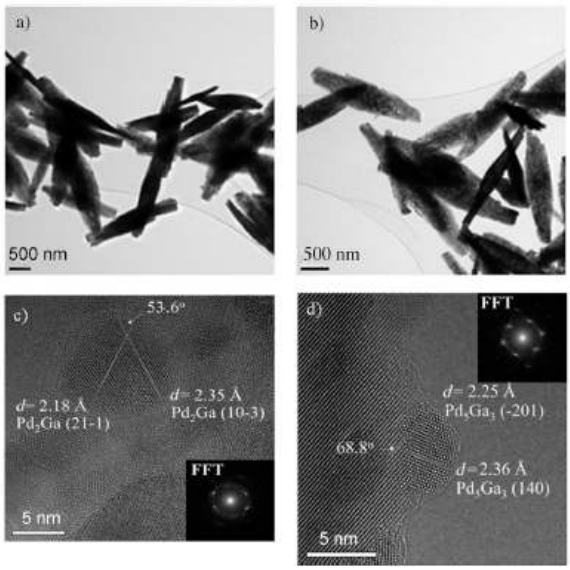

Figure 5. a,b) TEM and c,d) HRTEM of Pd_2Ga/a-Ga_2O_3 (a,c) and Pd_5Ga_2/a-Ga_2O_3 (b,d) prepared from PdO/a-Ga_2O_3 by reduction at 250 °C and 550 °C, respectively. Insets of parts c) and d) show the fast Fourier transform (FFT) analyses of the respective selected areas.

reduction of the Ga_2O_3 support to lower-valent Ga species. The lower reduction temperature compared to Ga_2O_3 without Pd is due to the ability of the IMCs to activate dihydrogen. Interestingly, the formation of Pd_2Ga seems not to proceed via PdH_x as has been reported in the case of the synthesis of unsupported Pd_2Ga nanoparticles[18] – most likely due to the higher temperature necessary for the reduction of Ga_2O_3 compared to $GaCl_3$, which is outside the stability range of PdH_x.

From XPS and TPR investigations, two reduction temperatures have been chosen for the PdO/a-Ga_2O_3 sample: 250 °C (reduction step 1) and 550 °C at the onset of reduction step 2. According to the experimental data the lower reduction temperature is just sufficient for formation of a Ga-Pd IMC, while the higher reduction temperature should yield a heavily reduced sample but without reductive decomposition of the gallia support. XRD patterns are shown in Figure 4. Peak positions of the a-Ga_2O_3 support remained unchanged regardless of reduction temperature and are marked by circles. Phase identification of the Ga-Pd IMCs is hardly possible by means of XRD alone, as only very weak and broad reflections can be detected, which is ascribed to the low total amount of Pd and the small particle size. In addition, the XRD patterns of different Ga-Pd phases show a rough similarity and overlap of strong reflections with those of the a-Ga_2O_3 support further prevent unambiguous assignment. However, the pattern of the IMC Pd_2Ga[34] seems to provide the best explanation for the experimentally observed scattered intensity in the region where the strongest peaks are expected (Fig. 4) for the sample reduced at lower temperature. The situation is more complicated for the higher reduction temperature, where no assignment is possible. High resolution TEM provides support for the phase Pd_5Ga_3[35] (see below), which is the next Ga-richer compounds in the Ga-Pd phase diagram.[36]

TEM, HAADF STEM and EDX elemental maps were used to characterize the crystal structure, the particle size and morphology of the Ga-Pd particles and the elemental distribution in the materials. TEM images in Figure 5 show the typical morphology of the PdO/α-Ga_2O_3 aggregates after reduction at low and high reduction temperature. It can be seen that the sample has basically conserved the initial morphology of the calcined precursor (Fig. 5a,b). The contrast fluctuations of the particles indicate a high porosity in agreement with the pore openings observed by SEM at the surface of the materials after calcination (Fig. 1a).

HAADF-EDX mapping (presented as supplementary data) indicates a homogeneous distribution of the elements suggesting a good dispersion and small particle size of most metal particles with the exception of a few larger Pd-rich particles. High resolution images (Fig. 5c, d) confirm the presence of spherical particles with an average size of around 5–8 nm for both reduction temperatures indicating a good stability against thermal sintering. From the Fourier transformed lattice fringes, the present phases could be identified as Pd_2Ga and Pd_5Ga_3, respectively, in agreement with TPR, XPS and XRD results.

The PdO/b-Ga_2O_3 and PdO/g-Ga_2O_3 samples have been subjected to similar TPR, XRD and TEM investigation and selected characterization results are presented in Table 2 (more detailed information can be found as supplementary data). The major difference between the two crystalline α-Ga_2O_3 and β-Ga_2O_3 supported samples was that the two TPR signal were found at slightly higher

Table 2. Characterization results for the reduced samples.

Calcined sample	T_{red} [°C]	BET-SA [m^2g^{-1}]	IMC phases[a]	IMC particle size[b] [(±3) nm]
PdO/α-Ga_2O_3	250	69	Pd_2Ga/Pd_5Ga_3	6
	550	27	Pd_5Ga_3/Pd_5Ga_3	5
PdO/β-Ga_2O_3	310	28	Pd_2Ga/Pd_5Ga_3	8
	565	27	$Pd_2Ga, Pd_5Ga_3/Pd_5Ga_3$	7
PdO/γ-Ga_2O_3	160	99	–[c]	–[c]
	500	88	–[c]	–[c]

[a] From XRD/TEM. [b] From TEM. [c] No IMC phase observed.

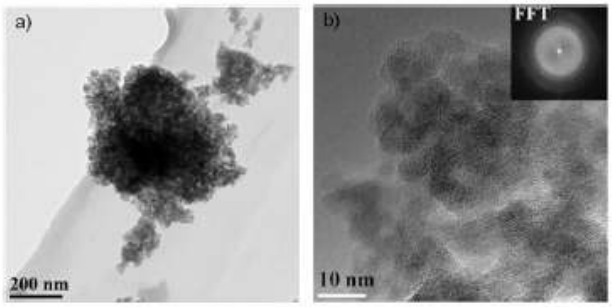

Figure 6. TEM (a), and HRTEM (b) images of the PdO/g-Ga_2O_3 sample reduced at 160 °C. The inset of part b) shows the corresponding FFT analysis.

temperature for the latter. The reduction temperatures have been adjusted to 310 and 565 °C accordingly. Otherwise, the same IMCs and similar particle sizes have been obtained, with the exception that small peaks of Pd_2Ga were still present in the XRD pattern of PdO/β-Ga_2O_3 reduced at 565 °C in addition to Pd_5Ga_3.

In case of the amorphous PdO/g-Ga_2O_3 sample, a different behavior has been observed. Three TPR peaks were detected at 144, 268 and 449 °C. 160 and 500 °C have been chosen as reduction temperatures. The amorphous structure, the highly aggregated g-Ga_2O_3 nanoparticles as well as the homogeneous distribution of Pd have been maintained during reduction (Fig. 6 and supplementary data). The Fourier transformed HRTEM image in Figure 6b shows no features that allow structural characterization of the gallia material or the Pd-containing phases for this sample.

2.3. Catalytic performance

Ga-Pd IMCs have been reported to be promising catalysts for selective hydrogenation,[1,9,10,14] methanol synthesis[37] and methanol steam reforming.[16,23,38,39] Dramatically different selectivities of the Ga-Pd catalysts compared with pure monometallic Pd have been reported in all cases and all three reactions have been conducted with selected Ga-Pd/gallia catalysts. The catalytically tested samples are summarized in Table 3.

2.3.1. Semi-hydrogenation of acetylene

Semi-hydrogenation of acetylene in a large excess of ethylene is an important step in the purification of the ethylene feed for the polyethylene production. Presence of acetylene leads to poisoning of the polymerization catalyst by adsorbing at the active sites for ethylene and blocks the polymerization process, so it must be reduced to a level less than 1 ppm.[40,41] It was demonstrated that palladium-based catalysts are extremely effective for selective hydrogenations.[42-46] Moreover, the Ga-Pd IMCs with the well-ordered crystal structure have been reported to exhibit high selectivity to the semi-hydrogenated product and long-term stability in acetylene hydrogenation. This has been related to the isolated active sites, the high structural stability, and absence of segregation or bulk-hydride formation.[1,9,14]

In this work, the selectivity of the Ga-Pd/gallia catalysts towards ethylene was determined in an excess of ethylene to confirm the formation of an intermetallic surface. Unmodified monometallic bulk-Pd[47] as well as Pd/Al_2O_3[1,12,14] are known to exhibit low selectivities to ethylene and to favor the total hydrogenation to ethane. First, all three catalysts have been reduced at the lower reduction temperature to obtain the IMC Pd_2Ga, and PdO/α-Ga_2O_3 additionally at 550 °C to obtain Pd_5Ga_3. Prior to the catalytic test, the samples were pretreated in 5% H_2 at the corresponding reduction temperature (Table 2). After purging the residual H_2 out of the reactor, the temperature was changed to 200 °C and the feed was switched to the ethylene-rich acetylene hydrogenation feed. Figure 7a and b show the conversion of acetylene and selectivity to ethylene during time-on-stream. A commercial Pd/Al_2O_3 catalyst (5 wt.-% Pd) purchased from Sigma-Aldrich is shown as a reference sample for monometallic Pd.

All tested catalysts do not reach a stable steady state conversion over 20 h on stream. In case of the catalysts reduced at lower reduction temperature, a slight decay of conversion is observed between beginning and end of the experiment. For the Pd_2Ga/gallia catalysts supported on the crystalline α- and β-Ga_2O_3 this decay was approximately 20 and 16% after 20 hours. Pd_2Ga/α-Ga_2O_3 showed an activity higher by roughly 11% compared to Pd_2Ga supported on β-Ga_2O_3. This is probably related to the higher specific surface area of the α-Ga_2O_3 support, which was calcined at lower temperature and to the slightly lower particle size of Pd_2Ga in this sample (Tab. 2). The Ga-Pd/γ-Ga_2O_3 catalyst shows an initial activity similar to the Pd_2Ga/β-Ga_2O_3 samples, but a strong deactivation in the first 6 hours TOS. After 20 hours TOS, the activity of the γ-Ga_2O_3 supported catalyst is only 35% and that of the β-Ga_2O_3-supported sample and approximately 80% of that of the α-Ga_2O_3-supported catalyst. In contrast, the Pd_5Ga_3/α-Ga_2O_3 catalysts reduced at high temperature shows an activation from 10 to 70 % conversion after 20 hours TOS, which is not near to finish at the end of the experiment. The amount of sample used was higher, so the activity should not be directly compared to the other three samples. Such an

Table 3. Sample overview and amounts used for catalytic tests.

Sample (T_{red} [°C])	Acetylene hydrogenation[a] [mg]	MSR[b] [mg]	Methanol synthesis from CO [mg]	Methanol synthesis from CO_2 [mg]
Pd_2Ga/α-Ga_2O_3 (250)	0.15	20	200	400
Pd_5Ga_3/α-Ga_2O_3 (550)	2.78	20	200	–
Pd_2Ga/β-Ga_2O_3 (310)	0.15	20	200	–
Pd_2Ga, Pd_5Ga_3/β-Ga_2O_3 (565)	–	20	200	–
Pd-Ga/γ-Ga_2O_3 (160)	0.15	20	200	–
Pd-Ga/γ-Ga_2O_3 (500)	–	20	200	–

[a] A commercial Pd/Al_2O_3 catalyst (0.1 mg, 5 wt% Pd, Sigma–Aldrich was used as reference catalyst. [b] A Pd/Al_2O_3 catalyst prepared by co-precipitation was used as reference catalyst (20 mg, see the Supporting Information for details).

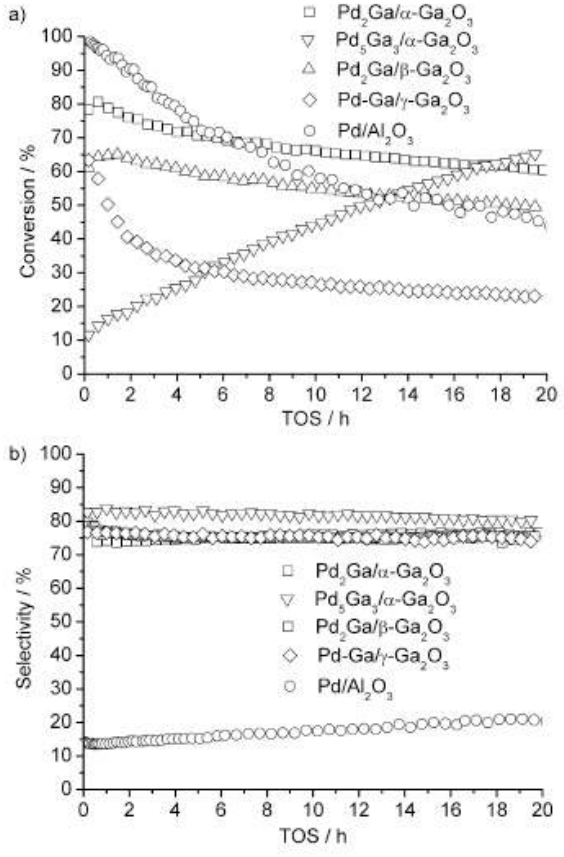

Figure 7. Comparison of the catalytic performances of different Ga-Pd/gallia catalysts in the semi-hydrogenation of acetylene. a) Conversions of acetylene and b) the selectivity towards ethylene. The catalyst masses and reduction temperature can be found in Table 3.

activation behavior has also been observed for Pd_2Ga catalysts prepared from hydrotalcite-like precursors.[19] and will be subject of further studies. The Pd/Al_2O_3 catalysts showed a strong deactivation under these conditions probably due to the formation of carbonaceous deposits at the Pd surface. Similarly, coking and green oil formation may also contribute to the observed deactivation of the Ga-Pd IMC catalysts.

The selectivities towards ethylene were between 74–77% for all gallia-supported samples reduced at lower temperature. These values are higher than that obtained for monometallic Pd (ca. 20%) and typical for the IMC Pd_2Ga.[10] This confirms that the IMCs have been formed, probably also in the γ-Ga_2O_3-supported sample. For the Pd_5Ga_3/α-Ga_2O_3 catalyst, a slightly but significantly higher selectivity of 80% has been detected suggesting that the change in IMCs composition is reflected in favorable intrinsic catalytic properties. Interestingly, the selectivities of all samples are relatively stable throughout the whole experiment, despite the considerable changes of conversion in particular of the Pd_2Ga/γ-Ga_2O_3 and Pd_5Ga_3/α-Ga_2O_3 catalyst. This may indicate that the change in conversion is rather related to an increased/decreased accessibility of the active IMCs particles than to a change of the active phase itself. Accessibility can be increased by changes in the metal-support-interaction after high temperature reduction[48] in case of Pd_5Ga_3/α-Ga_2O_3 or by breakdown of porosity of the amorphous support aggregates of Pd_2Ga/γ-Ga_2O_3 or coke formation[49] under reaction conditions.

2.3.2. Methanol steam reforming

Methanol steam reforming (MSR) yielding H_2 and CO_2 according to $CH_3OH + H_2O \rightarrow CO_2 + 3\ H_2$ is among the most promising processes for on-board hydrogen production for fuel cells.[50,51] Many studies have focused on Cu-based catalysts, mainly due to the extensive use of Cu-based catalysts in methanol synthesis and the activity of these catalyst formulations also in the formal reverse reaction MSR. Cu-catalysts suffer from some significant drawbacks, including deactivation, pyrophoricity, and high-temperature sintering.[50, 51] Pd and other group VIII metals are also active for the conversion of methanol. However, they tend to not be selective for the reforming reaction but rather catalyze the decomposition of methanol ($CH_3OH \rightarrow CO + 2\ H_2$), which generates large amounts of CO. CO is an undesired by-product, which poisons the downstream fuel cell catalyst. Thus, a high selectivity to CO_2 is a major goal of MSR catalyst development. Pd supported on ZnO, Ga_2O_3 and In_2O_3, instead of inert supports, has been reported to possess a high activity and selectivity to CO_2 comparable to state-of-the-art Cu/ZnO-based catalysts.[16,17,23,38,39] This increase in CO_2-selectivity has been related to IMCs formation.

Conversion of methanol and selectivity to CO_2 and CO were monitored versus time under isothermal condition at 250 °C with a MeOH:H_2O ratio of 1:1 at atmospheric pressure (Fig. 8). The catalysts were pretreated in 5% H_2 at the corresponding reductive temperature (Table 2) and purged with He. A Pd/Al_2O_3 catalyst was tested for comparison (for details on this sample, see supplementary information). As expected for elemental Pd, this catalyst was completely unselective to CO_2 and exclusively catalyzed methanol decomposition. It can be seen that the presence of Ga in the Pd_2Ga/gallia catalysts prepared at low reduction

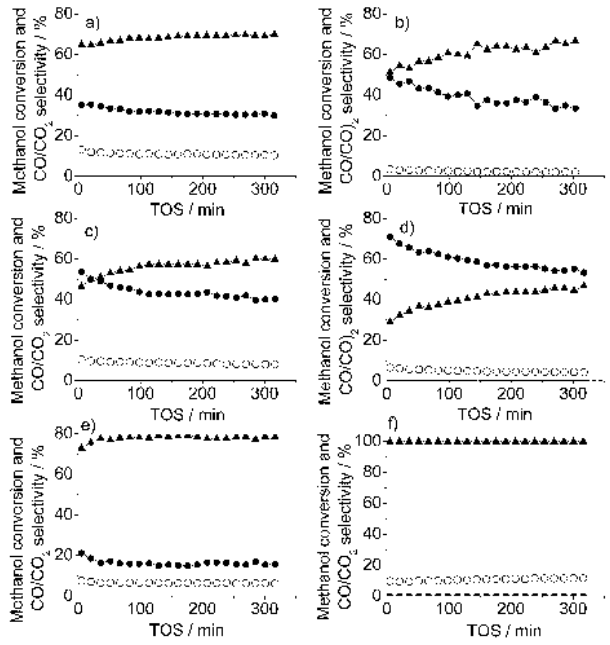

Figure 8. Methanol conversion (O) and CO (Δ), CO_2: (•) selectiveity in the MSR reaction with a) Pd_2Ga/α-Ga_2O_3, b) Pd_5Ga_3/α-Ga_2O_3, c) Pd_2Ga/β-Ga_2O_3 and d) Pd_2Ga,Pd_5Ga_3/β-Ga_2O_3, e) Ga-Pd/g-Ga_2O_3 reduced at 160 °C, and f) a Pd/Al_2O_3 reference.

temperatures generally favors the selectivity towards CO_2. In this reaction a marked effect of the gallia polymorph can be observed and the selectivity increases in the order γ-Ga_2O_3 (ca. 20%) < α-Ga_2O_3 (ca. 30%) < β-Ga_2O_3 (ca. 40%). In all cases, the increased CO_2 selectivity was rather stable after 2 hours time-on-stream and is assigned to the formation of the IMC Pd_2Ga, which modifies the catalytic properties of Pd metal. It is noted, however, that other authors[16,17] report selectvities of more than 80% for Pd_2Ga, which was not reached in this study. This is tentatively related to the difference in IMCs particle size of the catalysts presented here compared to those of the abovementioned studies, which give relatively sharp XRD peaks and are assumed to be significantly larger. This assumption is in agreement with an observation made in the Pd-Zn system, where a lower selectivity towards CO_2 was found for catalysts with a smaller particle size.[52] Another explanation for the lower selectivity might be the incomplete conversion of Pd metal to the IMCs, in particular for the g-Ga_2O_3-supported sample, which was reduced at very low temperature. The critical dependence of the selectivity in the MSR reaction on the pre-treatment conditions of Pd/Ga_2O_3 catalysts has been investigated in the work of, e.g., Iwasa et al.,[23] Haghofer et al.[17] and Lorenz et al.[39] These authors found high selectivities only after reduction at 400 to 500 °C, while lower temperatures yielded only moderate selectivities comparable to the values observed in this study. Reduction at even higher temperature of 700 °C can lead again to a decrease in selectity.[39] However, from our characterization results, we have no indication of incomplete reduction or residual metallic Pd after reduction. On the other hand, it has to be considered that already the presence of low amount of monometallic Pd may be responsible for a significant drop of the CO_2-selectivity. CO from methanol decomposition may then further decompose the intermetallic surface.[17] Thus, the selectivity in the MSR reactions might be taken as a sensitive measure for the ratio of monometallic and intermetallic Pd species in the catalysts. Assuming that a high CO_2-selectivity is an indicator for the intermetallic phase, our samples should contain a significant amount of monometallic Pd, which, as it cannot be identified in the freshly reduced catalysts, has probably formed by decomposition of the intermetallic phase under reaction conditions.

At high reduction temperatures, the IMC Pd_5Ga_3 was formed on the α- and at least partially on the β-Ga_2O_3 support. Interestingly, a significant increase in the initial CO_2 selectivity was observed, which is in agreement with literature reports and can be attributed to the formation of Ga-richer IMCs.[53] The highest selectivity towards CO_2 detected in this study was around 70% as the initial value for the Pd_5Ga_3/β-Ga_2O_3 catalyst. Unfortunately, this effect was not stable and vanished with time-on-stream. After 300 min on stream, the selectivity values previously observed for the low temperature reduced samples are reproduced for the α- and β-Ga_2O_3 supported catalysts after high temperature reduction. These results suggest that the Ga-richer Pd_5Ga_3 is not stable under MSR conditions. It might be converted back into Pd_2Ga, but also the Pd_2Ga surface has been recently reported to partially decompose under MSR conditions into monometallic Pd and oxidized gallia patches.[17] Such decomposition may be triggered by H_2O in the MSR feed or by CO in the product stream.[17] Our results indicate that the Ga-richer Pd_5Ga_3 phase might be even more sensitive to decomposition leading to a re-oxidation of Ga-species and yielding a state similar to that obtained after low temperature reduction.

The high temperature treatment goes hand-in-hand with a decrease in conversion. In case of the Pd/γ-Ga_2O_3, the catalyst is even mostly inactive after high temperature reduction (see supplementary information). This is most pronounced for the a-Ga_2O_3-suported catalysts and can be explained with the loss of surface area due to sintering of the support material as is seen from the BET data in Table 2 and/or to particle embedment due to strong metal support interaction at high reduction temperature. Sintering effects of the metal particles during sample pre-treatment can be excluded as no significant increase in metal particle size was detected by TEM after high temperature reduction.

2.3.3. Methanol synthesis

Methanol is an important base chemical and potential synthetic fuel. Industrial methanol synthesis is based on

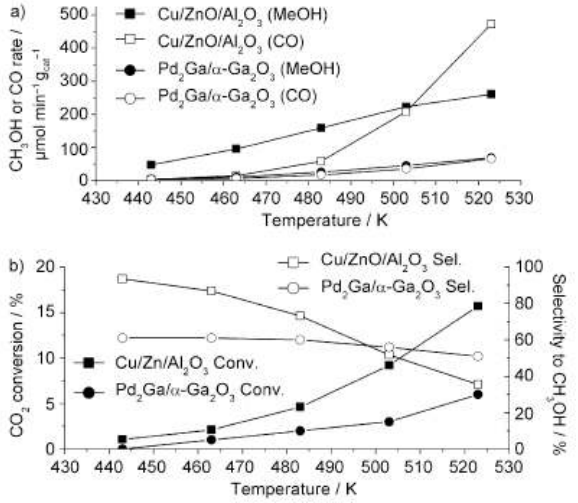

Figure 9. a) Methanol synthesis rates and b) selectivities of Pd_2Ga/α-Ga_2O_3 (•) and a $Cu/ZnO/Al_2O_3$ reference catalyst (■).

conversion of syngas ($H_2/CO/CO_2$) over $Cu/ZnO/Al_2O_3$ catalysts.[24,53,54] Pd has been considered as an alternative more active metal than copper and the activity and selectivity of Pd-based catalysts have been reported to depend on the type of metal oxide support, in which the metal-support interaction influences their structural and electronic character.[25,47,55-64] It is assumed that CO_2 is the major carbon source for methanol over Cu-based catalysts,[53] while on Pd it is produced from CO.[65] If CO_2/H_2 is used as a feed, methanol synthesis $CO_2 + 3\ H_2 \rightarrow CH_3OH + H_2O$ competes with the reverse water gas shift reaction (rWGS) $CO_2 + H_2 \rightarrow CO + H_2O$. We have carried out methanol synthesis from CO/H_2 ($CO:H_2$ = 1:1.7, 250 °C, 20 bar) and CO_2/H_2 ($CO_2:H_2$ = 1:3, 250 °C, 30 bar) mixtures to study the effect of IMCs formation on the catalytic properties.

After pretreatment in 5% H_2 at the corresponding reductive temperature (Pd/Ga_2O_3 reduced at high temperature is pretreated at 400 °C due to experimental limitations) and purging with Ar, the catalytic performance in CO hydrogenation over Pd-Ga/α-, β- and γ-Ga_2O_3 with low and high reductive temperature was measured and detailed results are reported in the supporting information. All catalysts are far less active and selective compared to conventional Cu-based catalysts. Only the Pd_2Ga/α-Ga_2O_3 reduced at 250 °C showed a significant selectivity to methanol at the beginning of the reaction but deactivates rather fast to 0% selectivity after 24 hours. All other catalysts did not produce methanol at any time from CO. Other products observed are mainly hydrocarbons due to the Fischer-Tropsch (F-T) reaction.[48] The same result was obtained for the monometallic Pd/Al_2O_3 reference catalysts showing that IMC formation did not have a clear beneficial effect on the catalytic properties of the catalysts in methanol synthesis from CO, which is probably related to the instability of the IMC surface in the presence of CO.[17]

In contrast to methanol synthesis from CO, the Pd_2Ga/a-Ga_2O_3 catalyst shows stable activity and good selectivity towards methanol synthesis from CO_2. The mass-normalized activities for methanol synthesis and the accompanying reverse water gas shift reaction from CO_2 hydrogenation are shown in Figure 9A for Pd_2Ga/a-Ga_2O_3 and a conventional $Cu/ZnO/Al_2O_3$ reference catalyst (see supporting information for more details on this sample). The Pd_2Ga/a-Ga_2O_3 catalyst shows only 20% of the activity of the mass normalized activity of the Cu-based catalyst at 230 °C, However, when the activity is normalized by active metal content (Pd and Cu respectively), the Pd_2Ga/a-Ga_2O_3 appears 5 times more active. From an Arrhenius plot of Figure 9A, apparent activation energies of 66 and 75 kJ/mol for methanol synthesis and rWGS are measured for the Pd_2Ga/a-Ga_2O_3. In comparison, the Cu based catalyst exhibits a similar apparent activation energy for methanol synthesis (53 kJ/mol) but a significantly higher apparent activation energy for rWGS (120 kJ/mol). As a result of these differences in apparent activation energies, the methanol selectivity of Pd_2Ga/a-Ga_2O_3 remains almost constant (50-60%) within the entire temperature range, whereas that of the copper-based catalyst increases drastically with decreasing temperature from 35 to 93% as shown in Figure 9B.

The presence of methanol synthesis activity during CO_2 hydrogenation on Pd_2Ga/a-Ga_2O_3 and its absence during CO hydrogenation are consistent with the findings of Iwasa et al.,[37] who attributed this behavior to the formation of Ga-Pd IMCs. Cu-based catalysts show a similar methanol synthesis activity behavior with respect to CO and CO_2 hydrogenation,[66] and CO_2 has been suggested as the carbon source for methanol formation on both catalysts. However, the differing apparent activation energies of rWGS between Cu-based and Pd intermetallic catalysts suggests mechanistic dissimilarities.

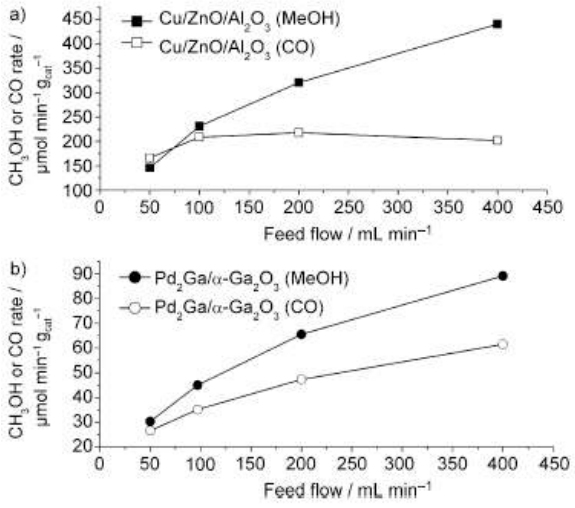

Figure 10. Flow rate variation studies on a) a $Cu/ZnO/Al_2O_3$ reference catalyst and b) Pd_2Ga/a-Ga_2O.

Further mechanistic differences in CO_2 hydrogenation between Cu and Pd based catalysts can be observed from the results of space velocity variation study as shown in Figure 10. Upon increasing the feed flow rate, the reaction products (H_2O, MeOH and CO) are diluted, whereas the concentration of reactants (CO_2 and H_2) remains nearly constant. In the absence of external mass transfer limitations, the effects of product inhibition can be indirectly observed. For the Cu-based catalyst (Figure 10A) the rate of methanol synthesis rises dramatically with increasing gas flow rate, suggesting strong product inhibition. The rate of rWGS, however remains nearly constant at flows greater than 50 ml/min (Figure 9B). Sahibzada et al.[66] showed that this behavior is related to the inhibition of methanol synthesis by water. In the case of Pd_2Ga/a-Ga_2O_3, the rates of rWGS and methanol synthesis both rise with increasing gas flow rate, suggesting that both rWGS and methanol synthesis are product inhibited.

3. Conclusion

A series of gallia-supported Ga-Pd catalysts that consists of metallic nanoparticles on three porous polymorphs of Ga_2O_3, α-, β- and γ-Ga_2O_3, has been synthesized by a controlled co-precipitation of Pd and Ga. The effect of formation of Ga-Pd IMCs has been studied in four catalytic reactions. The IMC Pd_2Ga forms upon reduction of α- and β-Ga_2O_3–supported materials in hydrogen at temperatures of 250 and 310 °C, respectively. At higher temperature Ga-enrichment of the intermetallic particles is observed leading to the formation of Pd_5Ga_3 before the support material is reduced at T > 565 °C. In the case of Ga-Pd/γ-Ga_2O_3 no direct information metal particles could be obtained due to a very small size and high dispersion, but the catalytic results suggest that the IMC Pd_2Ga also forms in this sample. The Pd_2Ga/gallia samples show a stable selectivity towards ethylene in acetylene hydrogenation around 75%, which is higher than expected for monometallic Pd catalysts. An even higher selectivity of 80% was observed for Pd_5Ga_3 supported on α-Ga_2O_3. In contrast to Pd/Al_2O_3, the Ga-Pd/gallia catalysts showed selectivity towards CO_2 in methanol steam reforming of up to 40%. However, higher selectivities that have been reported for Pd_2Ga in literature could not be reproduced in this study, which might be related to a particle size effect or incomplete IMC formation. The initially higher selectivity of the Pd_5Ga_3-containing samples was not stable suggesting superior catalytic properties of this IMC, but re-oxidation to Pd_2Ga under reaction condition. In methanol synthesis, no productivity from CO hydrogenation, but considerable methanol yield from a CO_2/H_2 feed has been observed for Pd_2Ga/α-Ga_2O_3.

In summary, Ga-Pd/Ga_2O_3 catalysts containing IMCs could be successfully synthesized. The effect of the different gallia polymorphs is small for α- and β-Ga_2O_3, but significant for γ-Ga_2O_3. The catalytic properties of Pd have been found to be positively affected by IMC formation for selective hydrogenation, methanol steam reforming and CO_2 hydrogenation, but no such effect was observed for CO hydrogenation.

Experimental Section

To prepare the Ga-Pd IMCs/α- and β-Ga_2O_3 polymorphs, their precursor was synthesized by controlled precipitation at pH 6 and temperature of 55 °C using co-feeding of appropriate amounts of 0.1 M mixed palladium and gallium nitrate (Ga:Pd = 98:2, molar ratio) solution and 0.345 M sodium carbonate solution as the precipitating agent. Both solutions were added simultaneously dropwise into a 2 L automated reactor, which was filled prior to the precipitation with bidistilled H_2O (300 mL).[67] The mixed nitrate solution was automatically pumped with a constant dosing rate (16 mL/min) and the sodium carbonate solution was added to maintain a constant pH. After completion of addition, the precipitates were aged for 24 h at the precipitation temperature under stirring. That whole process was conducted in a computer-controlled automated reactor system (Labmax, Mettler-Toledo). After filtration, the precipitate was washed twice with bidistilled water (400 mL). Then, the precipitate was dried at 80 °C in air for 12 h. The PdO/α- and β-Ga_2O_3 were produced by calcinations of the dried samples at 400 and 800 °C, respectively, in air for 2 h. Finally, to obtain the Ga-Pd IMCs, the reduction of Pd/α-Ga_2O_3 was performed in 5% H_2 at 250 and 550 °C; Pd/β-Ga_2O_3 was reduced by 5% H_2 at 310 and 565 °C.

To prepare the Ga-Pd IMCs/γ-Ga_2O_3 catalyst, 0.1 M mixed palladium and gallium nitrate (Ga:Pd = 98:2, molar ratio) solution and 0.345 M sodium carbonate solution as precipitating agent were added simultaneously dropwise into the 2 L reactor, prefilled with bidistilled H_2O (300 mL). While the dosing rate was unchanged, pH and temperature were lower compared with the preparation of the precursor for the Ga-Pd IMCs/α and β-phase (pH = 4, T = 25 °C). After completion of addition, the precipitate was directly filtered without aging and washed two times with ethanol (400 mL). Then, the precipitate was dried at room temperature (RT) in air for 3 days. The PdO/γ-Ga_2O_3 was produced by calcination of the dried samples at 500 °C in air for 2 h. Finally, to obtain the Ga-Pd IMCs, the reduction of Pd/γ-Ga_2O_3 was performed by 5% H_2 at 160 and 500 °C.

Acetylene hydrogenation was performed in a plug-flow stainless steel reactor with an inner diameter of 9 mm (PID & Engtech, MicroActivity). Activity, selectivity and long-term stability were investigated in a feed of 0.5% C_2H_2, 5% H_2 and 50% C_2H_4 in helium (total flow of 40 ml/min) at 200 °C isothermally for 20 h on stream. Reactant and product composition were analyzed with a Varian CP 4900 micro gas chromatograph. Methanol steam reforming (MSR) was carried out in a continuous fixed-bed flow reactor at 250 °C and atmospheric pressure in a flow of $CH_3OH:H_2O$ = 1:1. The product stream was analyzed by a HP6890 gas chromatograph, equipped with a HP plot Q

column, a nickel catalyst methanizer and a flame ionization detector. Methanol synthesis from CO was carried out at 250 °C and 2.0 MPa using H_2/CO gas mixtures in a stainless steel flow reactor. Gas phase analytic was done my means of gas chromatography. Methanol synthesis experiments involving CO_2 were also carried out in a stainless steel fixed bed flow reactor. The catalysts were reduced *in situ* at 523K (2 K/min) for 2 hours in 100 ccm (STP) of 20% H_2 in He. A 3:1 H_2/CO_2 mixture (100 mL/min) containing 4% Ar (as internal standard) was used to measure the catalytic activity at 523 K and 30 bar. Online analysis of products was performed with a GC (Agilent 6890). After the start of the reaction, the catalysts were allowed to stabilize for 4 hr time on stream. After this period, the activation energies of methanol synthesis and rWGS were measured in the temperature range of 463-548 K, with 2 hr allowed for each temperature point.

The characterization methods used and more experimental details on the catalytic measurements are described in the Supporting Information.

Acknowledgements

The doctoral student exchange program of the Chinese Academy of Sciences and the Max-Planck-Gesellschaft is acknowledged for a scholarship of L.L. Experimental help of Edith Kitzelmann, Frank Girgsdies, Gisela Lorenz, Gisela Weinberg and the ISISS team at BESSY-II is acknowledged. Many thanks are given to the COST Action CM0904 "Network for Intermetallic Compounds as Catalysts in the Steam Reforming of Methanol" for supporting the collaboration of the European groups.

References

[1] K. Kovnir, M. Armbrüster, D. Teschner, T. V. Venkov, F. C. Jentoft, A. Knop-Gericke, Y. Grin, R. Schlögl, Sci. Technol. Adv. Mater. 2007, 8, 420-427.
[2] B. Coq, F. Figueras, J. Mol. Catal. A: Chem. 2001, 173, 117-134.
[3] E. W. Shin, J. H. Kang, W. J. Kim, J. D. Park, S. H. Moon, Appl. Catal., A 2002, 223, 161-172.
[4] D. C. Huang, K. H. Chang, W. F. Pong, P. K. Tseng, K. J. Hung, W. F. Huang, Catal. Lett. 1998, 53, 155-159.
[5] P. A. Sheth, M. Neurock, C. M. Smith, J. Phys. Chem. B 2009, 109, 12449-12466.
[6] Y. M. Jin, A. K. Datye, E. Rightor, R. Gulotty, W. Waterman, M. Smith, M. Holbrook, J. Maj, J. Blackson, J. Catal. 2001, 203, 292-306.
[7] V. Ponec, Appl. Catal., A 2001, 222, 31-45.
[8] J. H. Kang, E. W. Shin, W. J. Kim, J. D. Park, J. Catal. 2002, 208, 310-320.
[9] J. Osswald, R. Giedigkeit, R. E. Jentoft, M. Armbrüster, F. Girgsdies, K. Kovnir, T. Ressler, Y. Grin, R. Schlögl, J. Catal. 2008, 258, 210-218.
[10] M. Armbrüster, K. Kovnir, M. Behrens, D. Teschner, Y. Grin, R. Schlögl, J. Am. Chem. Soc. 2010, 132, 14745-14747.
[11] K. Kovnir, M. Armbrüster, D. Teschner, T. V. Venkov, L. Szentmiklosi, F. C. Jentoft, A. Knop-Gericke, Y. Grin, R. Schlögl, Surf. Sci. 2009, 603, 1784-1792.
[12] K. Kovnir, J. Osswald, M. Armbrüster, D. Teschner, G. Weinberg, U. Wild, A. Knop-Gericke, T. Ressler, Y. Grin, R. Schlögl, J. Catal. 2009, 264, 93-103.
[13] J. Osswald, Active-Site Isolation for the Selective Hydrogenation of Acetylene: the Pd-Ga and Pd-Sn Intermetallic Compounds, Ph. D. Thesis, Technischen Universität Berlin, 2006.
[14] J. Osswald, K. Kovnir, M. Armbrüster, R. Giedigkeit, R. E. Jentoft, U. Wild, Y. Grin, R. Schlögl, J. Catal. 2008, 258, 219-227.
[15] L. D. Shao, W. Zhang, M. Armbrüster, D. Teschner, F. Girgsdies, B. S. Zhang, O. Timpe, M. Friedrich, R. Schlögl, D. S. Su, Angew. Chem. Int. Ed. 2011, 50, 10231-10235.
[16] N. Iwasa, T. Mayanagi, N. Ogawa, K. Sakata, N. Takezawa, Catal. Lett. 1998, 54, 119-123.
[17] A. Haghofer, K. Föttinger, F. Girgsdies, D. Teschner, A. Knop-Gericke, R. Schlögl, G. Rupprechter, J. Catal. 2012, 286, 13-21.
[18] M. Armbrüster, G. Wowsnick, M. Friedrich, M. Heggen, R. Cardoso-Gil, J. Am. Chem. Soc. 2011, 133, 9112-9118.
[19] A. Ota, M. Armbrüster, M. Behrens, D. Rosenthal, M. Friedrich, I. Kasatkin, F. Girgsdies, W. Zhang, R. Wagner, R. Schlögl, J. Phys. Chem. C 2011, 115, 1368-1374.
[20] L. D. Li, W. Wei, M. Behrens, Solid State Sci., *submitted*.
[21] N. Iwasa, S. Masuda, N. Ogawa, N. Takezawa, Appl. Catal., A 1995, 125, 145-157.
[22] N. Iwasa, T. Mayanagi, W. Nomura, M. Arai, N. Takezawa, Appl. Catal., A 2003, 248, 153-160.
[23] N. Iwasa, N. Takezawa, Top. Catal. 2003, 22, 215-224.
[24] Q. W. Zhang, X. H. Li, K. Fujimoto, Appl. Catal., A 2006, 309, 28-32.
[25] A. Gotti, R. Prins, J. Catal. 1998, 175, 302-311.
[26] M. Saito, S. Watanabe, I. Takahara, M. Inaba, K. Murata, Catal. Lett. 2003, 89, 213-217.
[28] S. Penner, B. Jenewein, K. Hayek, Catal. Lett. 2007, 113, 65-72.
[27] S. E. Collins, M. A. Baltanás, J. L. G. Fierro, A. L. Bonivardi, J. Cal. 2002, 211, 252-264.
[29] R. Carli, C. L. Bianchi, Appl. Surf. Sci. 1994, 74, 99-102.
[30] F. Scharmann, G. Cherkashinin, V. Breternitz, C. Knedlik, G. Hartung, T. Weber, J. A. Schaefer, Surf. Interface Anal. 2004, 36, 981-985.
[31] D. Briggs, M. P. Seah in Practical Surface Analysis (Second Edition) Volume 1: Auger and X-ray Photoelectron Spectroscopy, John Wiley, New York, 1990, pp. 609.
[32] E. S. Aydil, K. P. Giapis, R. A. Gottscho, V. M. Donnelly, E. Yoon, J. Vac. Sci. Technol., B: Microelectron. Nanometer Struct.—Process., Meas., Phenom. 1993, 11, 195-205.
[33] J. Shin, K. M. Geib, C. W. Wilmsen, P. Chu, H. H. Weider, J. Vac. Sci. Technol., A 1991, 9, 1029-1034.
[34] K. Kovnir, M. Schmidt, C. Waurisch, M. Armbrüster, Y. Prots, Y. Grin, Z. Kristallogr. – New Cryst. Struct. 2008, 223, 7-8.
[35] K. Schubert, H. L. Lukas, H. G. Meissner, S. Bhan, Z. Metallkd. 1959, 50, 534-540.
[36] H. Okamoto, J. Phase Equilib. Diffus. 2008, 29, 466-467.
[37] N. Iwasa, H. Suzuki, M. Terashita, M. Arai, N. Takezawa, Catal. Lett. 2004, 96, 75-78.

[38] S. Penner, H. Lorenz, W. Jochum, M. Stoger-Pollach, D. Wang, C. Rameshan, B. Klötzer, Appl. Catal., A 2009, 358, 193-202.
[39] H. Lorenz, S. Penner, W. Jochum, C. Rameshan, B. Klötzer, Appl. Catal., A 2009, 358, 203-210.
[40] M. P. McDaniel in Handbook of Heterogeneous Catalysis, 2nd Edition (Eds: G. Ertl, H. Knözinger, F. Schüth, J. Weitkamp), Wiley-VCH, Weinheim, 2008, pp. 3733-3792.
[41] H. Amold, F. Döbert, J. Gaube in in Handbook of Heterogeneous Catalysis, 2nd Edition (Eds: G. Ertl, H. Knözinger, F. Schüth, J. Weitkamp), Wiley-VCH, Weinheim, 2008, pp. 3266-3284.
[42] Q. W. Zhang, J. Li, X. X. Liu, Q. M. Zhu, Appl. Catal., A 2000, 197, 221-228.
[43] D. Duca, F. Frusteri, A. Parmaliana, G. Deganello, Appl. Catal., A 1996, 146, 269-284.
[44] M. L. Derrien, Stud. Surf. Sci. Catal. 1986, 27, 613-666.
[45] A. Molnar, A. Sarkany, M. Varga, J. Mol. Catal. A: Chem. 2001, 173, 185-221.
[46] M. García-Mota, B. Bridier, J. Pérez-Ramírez, N. López, J. Catal. 2010, 273, 92–102.
[47] D. Teschner, J. Borsodi, A. Wootsch, Z. Révay, M. Hävecker, A. Knop-Gericke, S. D. Jackson, R. Schlögl, Science, 2008, 320, 86-89.
[48] N. Tsubaki, K. Fujimoto, Top. Catal. 2003, 22, 325-335.
[49] A. Borodziński, G. C. Bond, Catal. Rev. – Sci. Eng. 2006, 48, 91-144.
[50] K. Föttinger, J. A. Van Bokhoven, M. Nachtegaal, G. Rupprechter, J. Phys. Chem. Lett. 2011, 2, 428-433.
[51] D. R. Palo, R. A. Dagle, J. D. Holladay, Chem. Rev. 2007, 107, 3992-4021.
[52] T. Conant, A. M. Karim, V. Lebarbier, Y. Wang, F. Girgsdies, R. Schlögl, A. Datye, J. Catal. 2008, 257, 64-70.
[53] G. C. Chinchen, K. Mansfield, M. S. Spencer, Chem. Tech. 1990, 20, 692-699.
[54] J. B. Hansen, P. E. H. Nielsen in Handbook of Heterogeneous Catalysis, 2nd Edition (Eds: G. Ertl, H. Knözinger, F. Schüth, J. Weitkamp), Wiley-VCH, Weinheim, 2008, pp. 2920-2949.
[55] S. H. Ali, J. G. Goodwin, J. Catal. 1998, 176, 3-13.
[56] Y. A. Ryndin, R. F. Hicks, A. T. Bell, Y. I. Yermakov, J. Catal. 1981, 70, 287-297.
[57] B. M. Choudary, K. Matusek, I. Bogyay, L. Guczi, J. Catal. 1990, 122, 320-329.
[58] K. P. Kelly, T. Tatsumi, T. Uematsu, D. J. Driscoll, J. H. Lunsford, J. Catal. 1986, 101, 396-404.
[59] F. Fajula, R. G. Anthony, J. H. Lunsford, J. Catal. 1982, 73, 237-256.
[60] M. L. Poutsma, L. F. Elek, P. A. Ibarbia, A. P. Risch, J. A. Rabo, J. Catal. 1978, 52, 157-168.
[61] R. F. Hicks, A. T. Bell, J. Catal. 1985, 91, 104-115.
[62] J. S. Rieck, A. T. Bell, J. Catal. 1986, 99, 278-292.
[63] J. S. Rieck, A. T. Bell, J. Catal. 1986, 99, 262-277.
[64] M. Ichikawa, Bull. Chem. Soc. Jpn. 1978, 51, 2268-2273.
[65] G. V. d. Lee, V. Ponec, Catal. Rev. – Sci. Eng. 1987, 29, 183-218.
[66] M. Sahibzada, I. S. Metcalfe, D. Chadwick, J. Catal. 1998, 174, 111-118.
[67] B. Bems, M. Schur, A. Dassenoy, H. Junkes, D. Herein, R. Schlögl, Chem. – Eur. J. 2003, 9, 2039-2052.